A versatile synthetic approach to design tailor-made push-pull chromophores with intriguing and tunable photophysical signatures

José L. Belmonte-Vázquez, Rebeca Sola-Llano, Jorge Bañuelos, Lourdes Betancourt-Mendiola, Miguel A. Vázquez-Guevara, Iñigo López-Arbeloa, Eduardo Peña-Cabrera*

http://dx.doi.org/10.1016/j.dyepig.2017.08.014

Dyes and Pigments 147 (2017) 246–259

A versatile synthetic approach to design tailor-made push-pull chromophores with intriguing and tunable photophysical signatures

José L. Belmonte-Vázquez,[a] Rebeca Sola-Llano,[b,*] Jorge Bañuelos,[b] Lourdes Betancourt-Mendiola,[a] Miguel A. Vázquez-Guevara,[a] Iñigo López-Arbeloa,[b] Eduardo Peña-Cabrera.[a,*]

[a] *Departamento de Química. Universidad de Guanajuato. Norial Alta S/N. Guanajuato, Gto. 36050, Mexico.*

[b] *Departamento de Química Física, Universidad del País Vasco-EHU, Apartado 644, 48080, Bilbao, Spain.*

E-mail: rebeca.sola@ehu.es, eduardop@ugto.mx

ABSTRACT. Novel modified Biellmann BODIPYs were prepared using a C-H arylation reaction with *in-situ* formed aryldiazonium salts. The post-functionalization of the methylthio group of these derivatives was demonstrated in S_NAr and the Liebeskind-Srogl cross-coupling reactions. The series of compounds herein designed with specific and selective functionalization featuring electron donor and acceptor groups provides valuable information about the impact of the molecular structure and stereoelectronic properties of the substituent on the photophysical signatures of BODIYs. In fact, push-pull dyes showing unexpected high fluorescence response towards the red edge of the visible spectrum can be designed, or, alternatively, chromophores ongoing the expected intramolecular charge transfer states (dark or fluorescent depending on the substituent, the attachment position and the surrounding media) can be also attained owing to the characteristic high charge separation of this king of dyes. We envisage that the reactivity of the selected scaffold as well as the guidelines derived from the computationally-aided spectroscopy study of these luminophores pave the way to the development of tailor made BODIPYs with specific and finely modulable spectroscopic and optical properties.

Keywords: BODIPY, push-pull dyes, organic synthesis, C-H activation, photophysical properties, charge transfer

1. Introduction

In 2006, Biellmann and coworkers reported the first 8-heteroatom-substituted BODIPY dyes **1a-c** (henceforth termed Biellmann BODIPYs) (Fig. 1) [1].

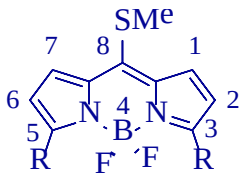

1a R = H, λ_{abs} = 527 nm, λ_{fl} = 539 nm
1b R = Me λ_{abs} = 530 nm, λ_{fl} = 554 nm
1c R = Et λ_{abs} = 523 nm, λ_{fl} = 544 nm

Fig. 1. Biellmann BODIPYs

Biellmann reported their photophysical properties in CH_2Cl_2 and carried out a brief study of their reactivity. This report became of significant importance since these building blocks demonstrated in the following years that new and previously inaccessible modes of reactivity for BODIPYs were available. This was of paramount relevance owing to the well-known properties and applications of these dyes [2]. The presence of the methylthio group in the 8-position, endows them with new modes of reactivity, for example, this group participates in S_NAr-like reactions allowing the introduction of nucleophiles such like alcohols, phenols, amines, phosphines, and 1,3-dicabonyl derivatives. Likewise, the MeS-group proved to be an excellent partner in Pd-catalyzed, Cu-mediated cross-coupling reactions (i.e., the Liebeskind-Srogl cross-coupling reaction, LSCC, with aryl, alkenyl, and heteroaryl boronic acids and organostannanes) [3]. Our group recently reported the synthesis of building block **2** that displayed orthogonal reactivity, demonstrating an increased versatility of the Biellmann BODIPYs (Fig. 2) [4]. Despite the rich functionality that could be introduced on **2a** and **2b**, it is always desirable to accomplish the same goal with the minimum modifications on the starting materials. In other words, a much more attractive possibility would be to start from Biellmann BODIPYs **1a-c** and be able to

introduce functional groups at the unsubstituted positions leaving the MeS-group intact, so that it could be modified according to the end purpose in mind, at a later stage of the synthesis.

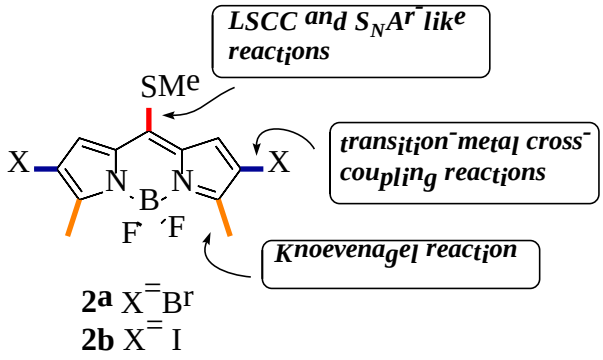

Fig. 2. Orthogonal reaction sites of BODIPYs **2a** and **2b**

Against this background, it is clear that the solution to this challenge would be the selective C-H functionalization of **1a-c**. There are just a few methods reported in the literature that describe the C-H activation of BODIPYs. For example, Burgess introduced an electron-withdrawing vinyl group at the 2-position by treating 2-unsubstituted BODIPY dyes with activated double-bonds, a Pd(II) catalyst, and an oxidant [5], whereas Dehaen and co-workers described both a radical C-H arylation of BODIPYs with aryldiazonium salts [6], and a radical C-H alkylation of the same dyes with potassium trifluoroborates [7] (Scheme 1).

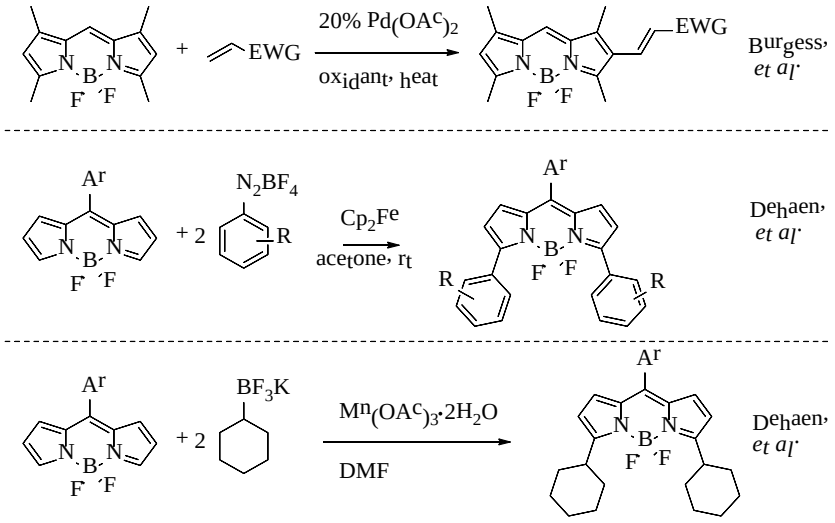

Scheme 1. Reported examples of C-H activation reaction on the BODIPY core

Building upon Dehaen´s results, we envisioned the C-H arylation of **1a** and **1b** in order to functionalize the 3- and 1-positions respectively. Thus, by extending the conjugation of the BODIPY core, one would obtain Biellmann BODIPYs that absorb and emit towards lower energies of the visible spectrum, from which it would be possible to manipulate the methylthio group by using the aforementioned reactions (Fig. 3).

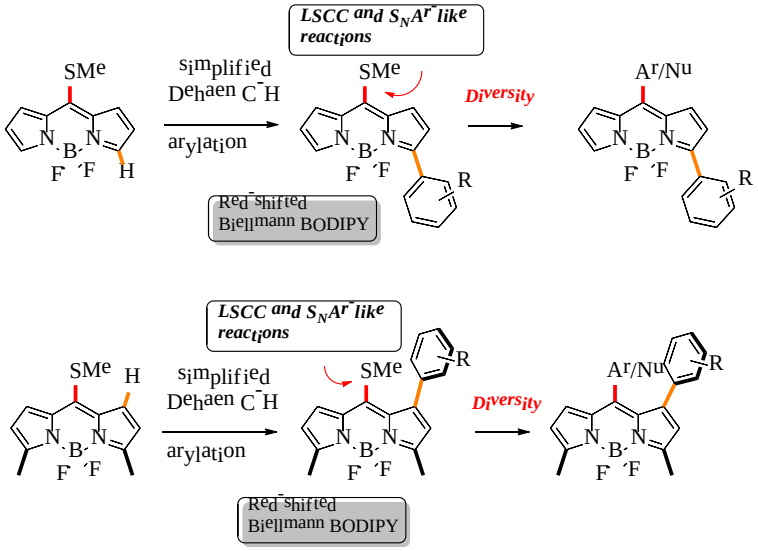

Fig. 3. Synthesis and functionalization of Biellmann BODIPYs that absorb and emit towards the red region of the visible spectrum.

Why would the possibility to obtain BODIPY-based fluorophores that absorb and emit towards the less energetic end of the visible spectrum be relevant? As a large number of publications mention, BODIPYs that fluoresce in the NIR region of the spectrum (650-900 nm), find numerous biology-related applications since light in this region causes almost no damage to bio-tissues, reaches deep tissue penetration, and causes minimum auto-absorption and auto-fluorescence from biomolecules [8]. Likewise, there are reports in the literature that describe the applications of NIR BODIPYs as NIR-photosensitizers for potential applications such as heat absorbers, NIR light-emitting diodes, and solar cells [9]. Understanding the variables that control the photophysical properties of the products studied herein, would allow for the design of new BODIPY-based fluorophores that absorb and emit in the NIR region.

The rich and selective functionalization of the dyes developed by the above claimed synthetic methodology (Fig. 3) provides an excellent background to gather such valuable information about the impact of the substitution pattern (electron donor and acceptors, or the combination of both in a single fashion, as well as the linkage chromophoric positions) on the photophysical signatures of BODIPY. As a result, push-pull chromophores in which opposite functionalities, electron donor (ED, such as amine derivatives, methoxy or thiomethyl) and withdrawing (EW, such as nitro, carboxilate or halogen motifs) groups are simultaneously placed in the same dipyrrin backbone (but at different positions, 3-8 or 1-8) have been designed [10]. This kind of chromophores are deserving of much attention in the last years owing to their inherent charge separation which enables to apply BODIPYs for instance in dye sensitized solar cells (DSSC) [11], and in non-linear optics (NLO) [12], such as two-photon absorption (TPA) [13]. Along the following lines we intend to provide key guidelines to understand the intriguing photophysical properties of the herein tested

dyes as well as to orient the synthesis of future smart dyes with tailor-made properties. To this aim, the reactivity as well as the photophysical properties, supplemented by quantum mechanics calculations, are thoroughly described. It is noted that the fluorescence response of most of the tested BODIPYs is triggered by the charge transfer processes induced by the presence of ED and EW moieties decorating the dipyrrin core, which usually render an effective fluorescence quenching depending on the environmental polarity. However, strikingly high fluorescence signals can be recorded towards the red-edge by choosing an adequate combination of ED and EW groups at suitable chromophoric positions.

2. Experimental

2.1. Synthetic Procedures

2.1.1.General procedure for C-H activation on the 3-position (GP1).

An oven-dried two-necked flask equipped with a stir bar was charged with methylthioBODIPY **1a** (5.0 equiv), the corresponding aniline derivative (1.0 equiv), and dry CH_3CN (0.003 M). The mixture was stirred until the solids dissolved. *t*-BuONO (1.5 equiv) was then added with a syringe. A fine bubbling was observed thereafter. The reaction was kept at room temperature until no changes in the TLC were observed (TLC 30 % EtOAc/hexanes). Excess of solvent was removed under vacuum and the crude material was adsorbed in SiO_2-gel. The product was purified by flash chromatography on SiO_2-gel using THF/hexanes as eluent.

2.1.2.General procedure for C-H activation at the 3- and 5-positions (GP2).

An oven-dried two-necked flask equipped with a stir bar was charged with methylthioBODIPY **1a** (1.0 equiv), the corresponding aniline derivative (5.0 equiv), and

dry CH_3CN (3 mL). The mixture was stirred until the solids dissolved. *t*-BuONO (7.5 equiv) was then added with a syringe. A fine bubbling was observed thereafter. The reaction was kept at room temperature until no changes in the TLC were observed (TLC 30% EtOAc/hexanes). The crude material was adsorbed in SiO_2-gel and the product was purified by flash chromatography on SiO_2-gel using THF/hexanes as eluent.

2.1.3. General procedure for the C-H activation on the 1 position (GP3).

An oven-dried two-necked flask equipped with a stir bar was charged with 3,5-dimethyl-8-methylthioBODIPY **1b** (5.0 equiv), the corresponding aniline derivative (1.0 equiv), and dry CH_3CN (10 mL). The mixture was stirred until the solids dissolved. *t*-BuONO (1.5 equiv) was then added with a syringe. A fine bubbling was observed thereafter. The reaction was kept at room temperature until no changes in the TLC were observed. (TLC 30 % EtOAc/hexanes). Excess of solvent was removed under vacuum and the crude material was adsorbed in SiO_2-gel. The product was purified by flash chromatography on SiO_2-gel using THF/hexanes as eluent.

2.1.4. General Procedure for the L−S Cross-Coupling reaction (GP4).

A Schlenk tube equipped with a stir bar was charged with **6** (1.0 equiv), the corresponding boronic acid (3.0 equiv), and dry THF (0.03 M). The mixture was sparged with N_2 for 3 min, whereupon $Pd_2(dba)_3$ (2.5 mol %), trifurylphosphine (7.5%), and CuTC (3.0 equiv) were added under N_2. The Schlenk tube was then immersed in a preheated oil bath at 55 °C. The oil bath was removed after the starting BODIPY was consumed (TLC, 20% THF/ hexanes). After the mixture reached rt, the solvent was removed, the crude material was adsorbed in SiO_2 gel, and then purified by flash chromatography on SiO_2 gel using THF/hexanes as eluent.

2.1.5. General Procedure for the reduction reaction using 5% Pd/C (GP5).

A round bottom flask equipped with a stir bar was charged with the corresponding BODIPY (1.0 equiv), then a mixture of MeOH/THF [1:1, (2.4 mL)] and 5% Pd/C (5.0 equiv) was added. After purging with N_2, hydrazine monohydrate (22 equiv) was added. The solution was stirred at refluxed under N_2 (20 - 45 min). The oil bath was removed after the starting BODIPY was consumed (TLC, 20% THF/hexanes). After the mixture reached rt, the solvent was removed and the crude material was adsorbed in SiO_2 gel, and then purified by flash chromatography on SiO_2 gel using THF/hexanes or EtOAc/hexanes as indicated.

2.2. Spectroscopic Techniques

Diluted dye solutions (around $4 \cdot 10^{-6}$ M) were prepared by adding the corresponding solvent (spectroscopic grade) to the residue from the adequate amount of a concentrated stock solution in acetone, after vacuum evaporation of this solvent. UV-Vis absorption and steady-state fluorescence were recorded on a Varian model CARY 7000 spectrophotometer and an Edinburgh Instruments spectrofluorimeter (model FLSP920), respectively, using 1 cm path length quartz cuvettes. The emission spectra were corrected from the monochromator wavelength dependence, the lamp profile and the photomultiplier sensitivity. Fluorescence quantum yields (ϕ) were calculated using commercial BODIPYs as reference: PM597 (ϕ^r = 0.43 in ethanol) for compounds **3-6**, **8** and **12-23**; PM650 (ϕ^r = 0.099 in ethanol) for compound **7**; and coumarin 152 (ϕ^r = 0.20 in ethanol) for compounds **9-11**. The values were corrected by the refractive index of the solvent. Radiative decay curves were registered with the time correlated single-photon counting technique using the same spectrofluorimeter (Edinburgh Instruments, model FL920, with picosecond time-

resolution). Fluorescence emission was monitored at the maximum emission wavelength after excitation by means of a pulsed Fianium Supercontinuum laser at an appropriate wavelength for each compound, with 150 ps full width at half maximum (FWHM) pulses. The fluorescence lifetime (τ) was obtained after the deconvolution of the instrumental response signal from the recorded decay curves by means of an iterative method. The goodness of the exponential fit was controlled by statistical parameters (chi-square) and the analysis of the residuals. Radiative (k_{fl}) and non-radiative (k_{nr}) rate constants were calculated as follows; $k_{fl} = \phi / \tau$ and $k_{nr} = (1-\phi)/\tau$.

2.3. Theoretical Simulations

Ground state geometries were optimized at the Density Functional Theory (DFT) level using the B3LYP hybrid functional. The Franck-Condon absorption simulation and first singlet excited state optimization was carried out by the Time-Dependent (TD-DFT) method. In all cases the double valence basis set adding a diffuse and polarization function (6-31+g*). The only exception is the iodo compound **5**, where the specific base for heavy atoms landl2dz had to be used. The energy minimization was conducted without any geometrical restriction and the geometries were considered as energy minimum when the corresponding frequency analysis did not give any negative value. The charge distribution was simulated by the CHelpG method. The solvent effect (cyclohexane) was also simulated during the calculations by the Self Consistent Reaction Field (SCRF) using the Polarizable Continuum Model (PCM). All the theoretical calculations were carried out using the Gaussian 09 implemented in the computational cluster provided by the SGIker resources of the UPV/EHU.

3. Results and Discussion

3.1. Synthesis

The starting point of this work was to test on Biellmann BODIPY **1a** the experimental conditions described by Dehaen and co-workers for the C-H arylation of 8-(2,6-dichlorophenyl)BODIPY **4**, to wit, ArN_2BF_4, ferrocene, acetone, rt. In sharp contrast with the results observed using BODIPY **4**, these conditions gave only complex mixtures of unreacted **1a**, plus varying amounts of the 3-aryl and 3,5-diaryl-subtituted products, regardless of the amount of the aryldiazonium salt used. A more detailed study of the best experimental conditions ensued (Table 1). Searching for reaction conditions that would not involve a separate synthesis of the potentially explosive diazonium salts [14], we turned our attention to the best results published by Carrillo and co-workers [15]. They describe the effectiveness of ascorbic acid as initiator for the C-H arylation of (hetero)arenes with in-situ formed diazonium salts. Indeed, these conditions gave the desired product with a 57% conversion (entry 3). However, it was observed that a higher conversion (62%) was obtained in the absence of ascorbic acid using *t*-BuONO as nitrosating agent (entry 2). Other nitrosating agents such as *i*-amyl nitrite or sodium nitrite resulted ineffective with or without ascorbic acid (entries 1, 4, 5, 6, 7, and 8). Using DMSO instead of acetonitrile was detrimental for the reaction and a very low conversion was observed (entries 8 and 9). On the other hand, good conversion (63%) was observed with the preformed BF_4^- diazonium salt (entry 10). The reaction did not proceed in the dark, suggesting that light was needed to form the free-radicals.

Table 1.

Survey of experimental conditions for the C-H arylation of BODIPY **1a**.

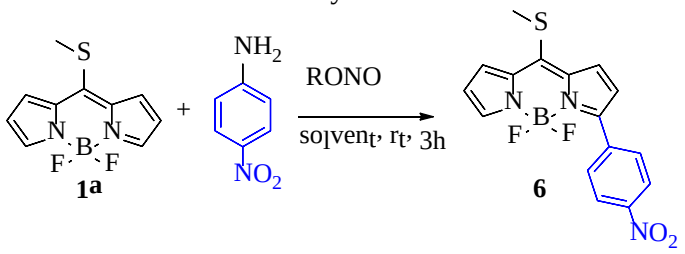

Entry	Initiator	Nitrosating agent	Solvent	Conversion (%)[a]
1	ascorbic acid[e,f]	*i*-AmONO	CH_3CN	-[c]
2	-	*t*-BuONO	CH_3CN	62
3	ascorbic acid[e,f]	*t*-BuONO	CH_3CN	57
4	-	NaONO	CH_3CN	-[d]
5	ascorbic acid[e,f]	NaONO	CH_3CN	-[d]
6	ascorbic acid[e]	*i*-AmONO	CH_3CN	12
7	-	*i*-AmONO	CH_3CN	9
8	-	*t*-BuONO	DMSO	2
9	ascorbic acid[e]	*t*-BuONO	DMSO	8
10	-	BF_4 diazonium salt	DMSO	63
11	ascorbic acid[e]	BF_4 diazonium salt	CH_3CN	15
12[b]	-	*t*-BuONO	CH_3CN	-[c]

[a]Conversion was measured using HPLC. [b]The reaction was carried out in the dark. [c]No reaction was observed. [d]Several products were obtained. [e]10% Ascorbic acid was used. [f]Ascorbic acid was dissolved in DMSO (0.05 M) before it was added.

Having demonstrated that no radical initiator was required and that the diazonium salt was generated in situ, we proceeded to explore the scope and limitations of this process (Chart 1).

Chart 1.

C-H activation at the 3-position

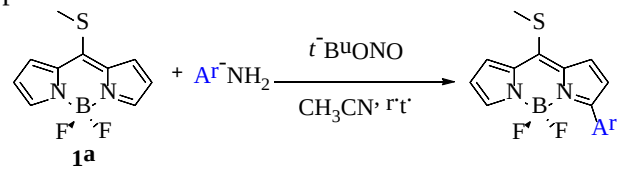

1a

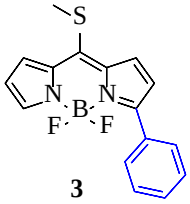 **3** 19%, 1h	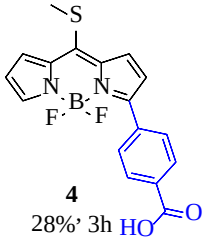 **4** 28%, 3h	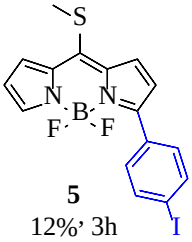 **5** 12%, 3h
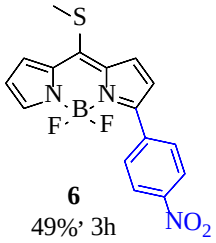 **6** 49%, 3h	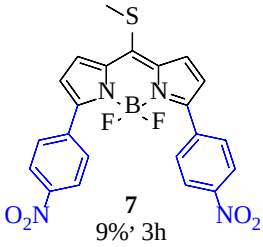 **7** 9%, 3h	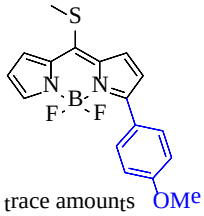 trace amounts

Disappointingly, the reaction gave modest to poor yields. However, the fact that all of them displayed interesting photophysical properties, including bathochromic shift, warranted the study of further transformations on both the *meso*-position and the 3-aryl substituent. According to the observations made by Dehaen [6], the reaction also failed when an electron-rich amine was used. The arylation reaction was also attempted on BODIPY **1b** (ec. 1), resulting in substitution at the 1-position.

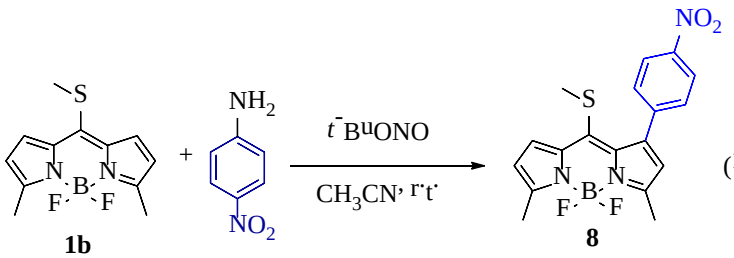

1b **8** 37%, 1h (1)

We then further proceeded to study the post-functionalization of the modified Biellmann BODIPYs. Thus, BODIPY **6** was subjected to the S_NAr reactions our groups have previously reported (Chart 2) [4].

Chart 2.
Application of the S_NAr reaction in the synthesis of *meso*-substituted BODIPY Analogues using the Biellmann BODIPY **6.**

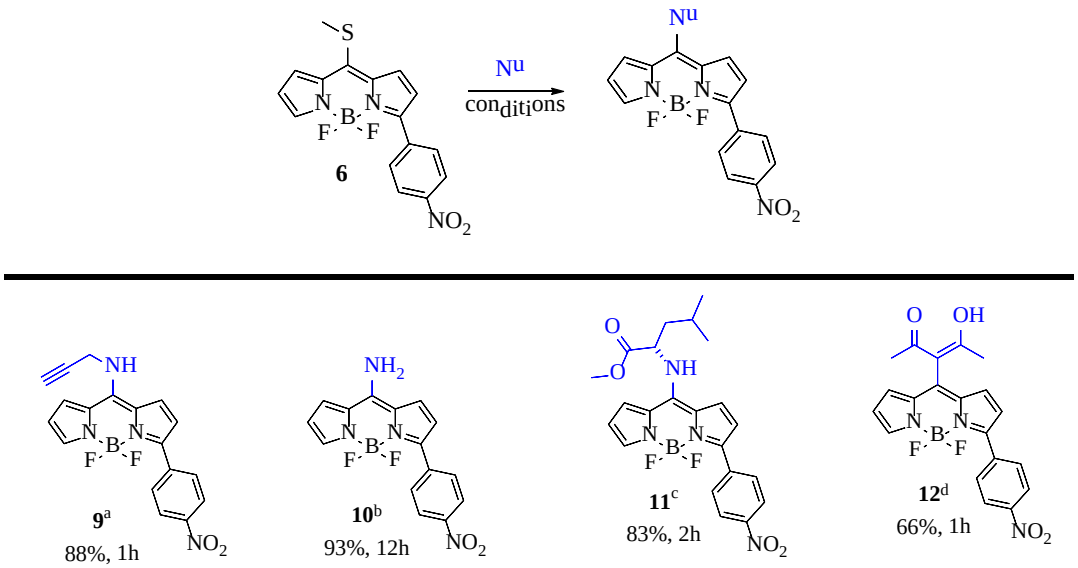

Conditions: [a]**6** (1 equiv), propargylamine (1.5 equiv), 1.5 mL of CH_3CN at r. t. [b]**6** (1 equiv), NH_4OAc (6 equiv), mixture H_2O/MeOH (1:1 v/v) at 60 °C overnight. [c]**6** (1 equiv), *L*-leucine methyl ester hydrochloride (1.5 equiv), 2.0 mL of CH_2Cl_2, TEA (1.5 equiv). [d]**6** (1 equiv), CuTC (1.1 equiv), DMSO (2.5 mL), acetylacetone (2.0 equiv) and Na_2CO_3 (2.0 equiv).

Addition of amines took place readily to produce the corresponding amino-derivatives in excellent yields, including *L*-leucine methyl ester. Acetilacetonate (acac) anion smoothly added to give 8-acac-BODIPY in moderate yield after 1 h.

Next, the reactivity of **6** in the Liebeskind-Srogl cross-coupling reaction was evaluated (Chart 3) [16].

Chart 3.
Application of the Liebeskind−Srogl Cross-Coupling reaction in the synthesis of *meso*-substituted BODIPY analogues using the Biellmann BODIPY **6.**

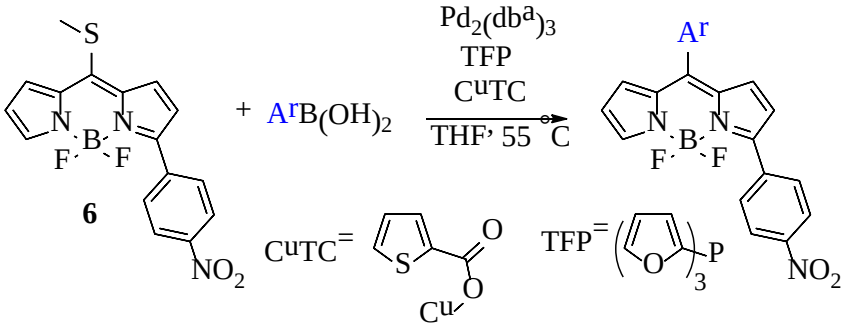

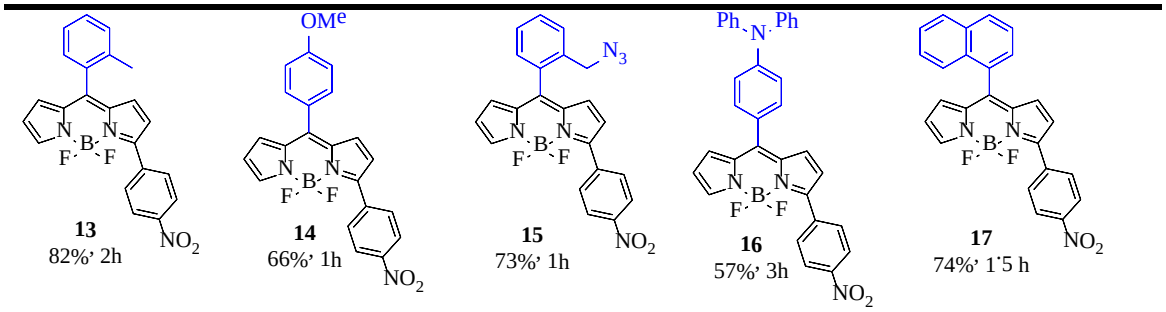

Conditions: **6** (1 equiv), $ArB(OH)_2$ (3 equiv), $Pd_2(dba)_3$ (2.5%), TFP (7.5%), CuTC (3 equiv), 55 °C, 0.03 M.

BODIPY **6** displayed excellent reactivity in the Liebesking-Srogl cross-coupling reaction. Products **13-17** were obtained in moderate to good yields in short reaction times. Encumbered boronic acids (utilized for products **13**, **15**, and **17**) reacted with similar reaction times to those with no *o*-substituent (for products **14** and **16**).

The reactivity of Biellmann BODIPY **8** was also evaluated in this type of cross-coupling (Chart 4).

Chart 4.

Reactivity of Biellmann BODIPY **8** in the Liebeskind−Srogl Cross-Coupling reaction.

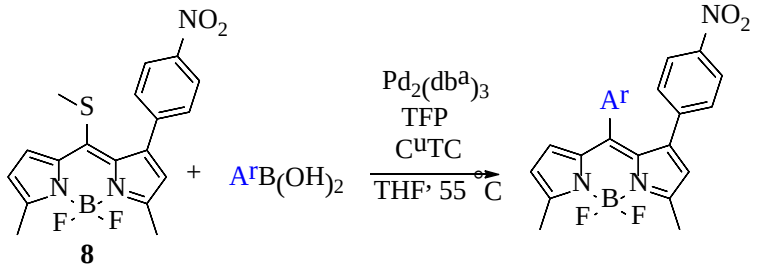

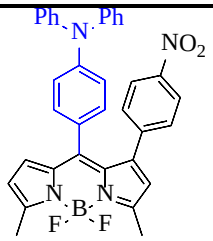

18, 81%, 2h

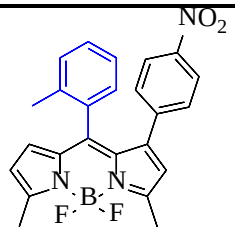

19, 54%, 2h

Typical Liebeskind-Srogl reaction conditions: 8 (1 equiv), $ArB(OH)_2$ (3 eq), $Pd_2(dba)_3$ (2.5%), TFP (7.5 %), CuTC (3 eq), 55 °C, 0.03 M.

Similar to the results observed in Chart 3, products **18** and **19** were obtained in moderate to good yields in comparable reaction times despite the fact that the reactive *meso*-position in **8** is more sterically encumbered as compared to **6**.

Finally, the nitro group of some of the derivatives prepared was reduced (Chart 5) [17]. The reduction of the nitro group took place smoothly to generate the corresponding anilines in good to excellent yields. No significant difference was observed when the nitrophenyl group was either at the 1- or 3-position.

Chart 5.

Reduction of the nitro group in some of the modified Biellmann BODIPYs prepared

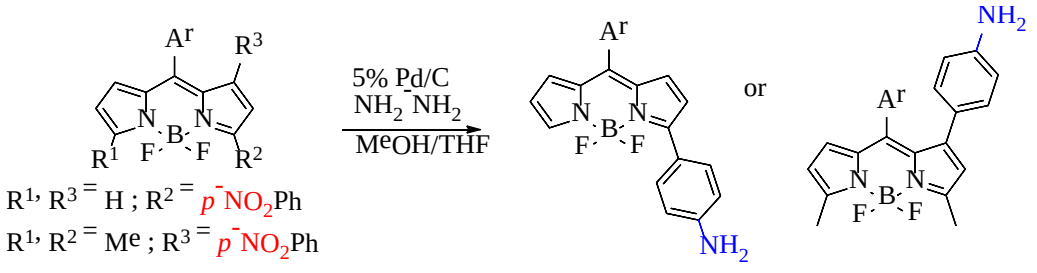

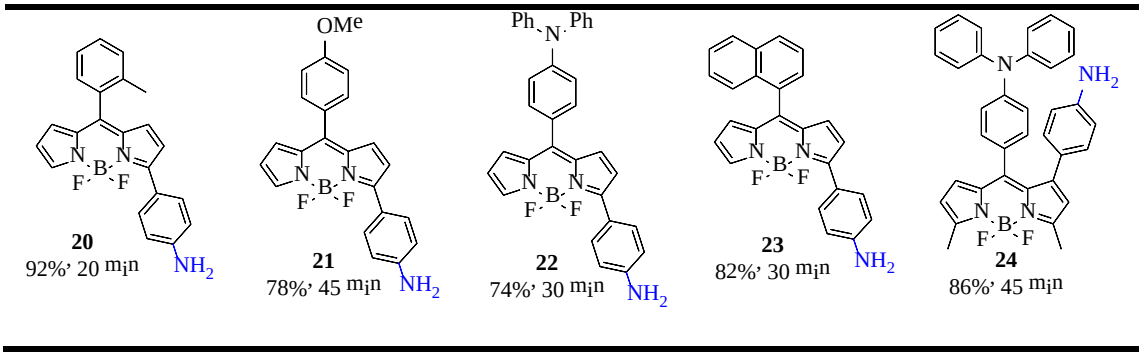

Reaction conditions: Starting BODIPY (1 equiv), [Pd/C] (5 equiv), hydrazine monohydrate (22 equiv), MeOH/THF [1:1, 2.4 mL] at reflux.

3.2. *Photophysical properties*

In view of the wide diversity of compounds attained (see above charts with different ED and EW groups combined at different chromophoric positions) we decided to classify them according to their molecular structure for a smoother and better understanding of the impact of such substitution patterns on the photophysical signatures.

*3.2.1. Dyes **3-7**: 3-substituted 8-methylthioBODIPYs*

In a previous work we characterized the spectroscopic properties of the reference dye **1a** [18]. The electron coupling of the ED 8-thiomethyl (Hammet parameter [19] σ_p^+ = -0.60) with the dipyrrin promoted the formation of a new hemicyanine-like resonant structure. Accordingly, it altered the absorption profile given rise to a broad band (full width at half maximum, fwhm, around 2000 cm^{-1}) as result of the contribution at higher

energies of such new hemicyanine mesomeric structure, plus the typical cyanine one of BODIPY at lower energies. The statistical weight of each resonant structure to the whole band depended on the alkylation pattern of the dipyrrin, as well as on the solvent polarity. However, the fluorescence profile was ruled just by the latter cyanine-like mesomeric form, giving a sharper and narrower band (fwhm around 1000 cm^{-1}), typical of BODIPY. Therefore, **1a** displayed a quite high fluorescence response (up to 75%) [18]. Besides, high Stokes shifts were achieved mainly in polar media (up to 1800 cm^{-1}), where the new hemicyanine-like mesomeric form resulting from the electronic coupling of the 8-methylthio group prevailed in the absorption spectrum.

The arylation at 3-position of **1a** renders dye **3** (see Chart 1), whose spectral bands are bathochromically shifted (Table 2) as result of the expected resonance interaction (feasible since the twisting dihedral angle is around 35º) which extends the delocalized π-system, mainly in the HOMO (Fig. 4). However, both the fluorescence quantum yield and lifetime decrease, especially in polar media (down to 15% with 1.36 ns in acetonitrile, Table 2), suggesting that such 3-aryl activates an extra non-radiative relaxation channel. A closer inspection to the frontier orbitals involved in the main electronic transition (from HOMO to LUMO as predicted by TD-DFT calculations) reveals that the excitation entails electronic density transfer from the phenyl (slightly ED, σ_p^+ = -0.18) to the dipyrrin core. Therefore, the locally excited (LE) state, whose geometry remains similar to that of the ground state, acquires some charge transfer character and anticipates the predisposition to populate from such state a low-lying and non-emissive photoinduced intramolecular charge transfer (ICT) state, which explains the sensibility of the fluorescence parameters to the solvent properties.

Table 2.

Photophysical data of dyes **3-7** in apolar (cyclohexane, c-hex) and polar (acetonitrile, ACN) media. Full photophysical data are collected in Table S1 in Supporting Information.

		λ_{ab}[a] (nm)	ε_{max}[b] $\cdot 10^{-4}$ ($M^{-1}cm^{-1}$)	λ_{fl}[c] (nm)	ϕ[d]	τ[e] (ns)
3	c-hex	541.0	6.2	568.0	0.34	2.82
	ACN	517.0	4.5	564.5	0.15	1.36
4	c-hex	540.5	6.0	572.5	0.57	4.54
	ACN	518.0	5.0	568.5	0.34	2.95
5	c-hex	544.5	5.9	577.0	0.53	3.96
	ACN	519.5	4.9	570.5	0.30	2.39
6	c-hex	534.0	4.7	572.5	0.72	5.37
	ACN	517.5	4.0	571.5	0.52	4.24
7	c-hex	567.5	4.1	614.5	0.73	5.91
	ACN	548.5	2.8	622.5	0.66	5.96

[a]Absorption wavelength. [b]Molar absorption. [c]Fluorescence wavelength. [d]Fluorescence quantum yield. [e]Fluorescence lifetime.

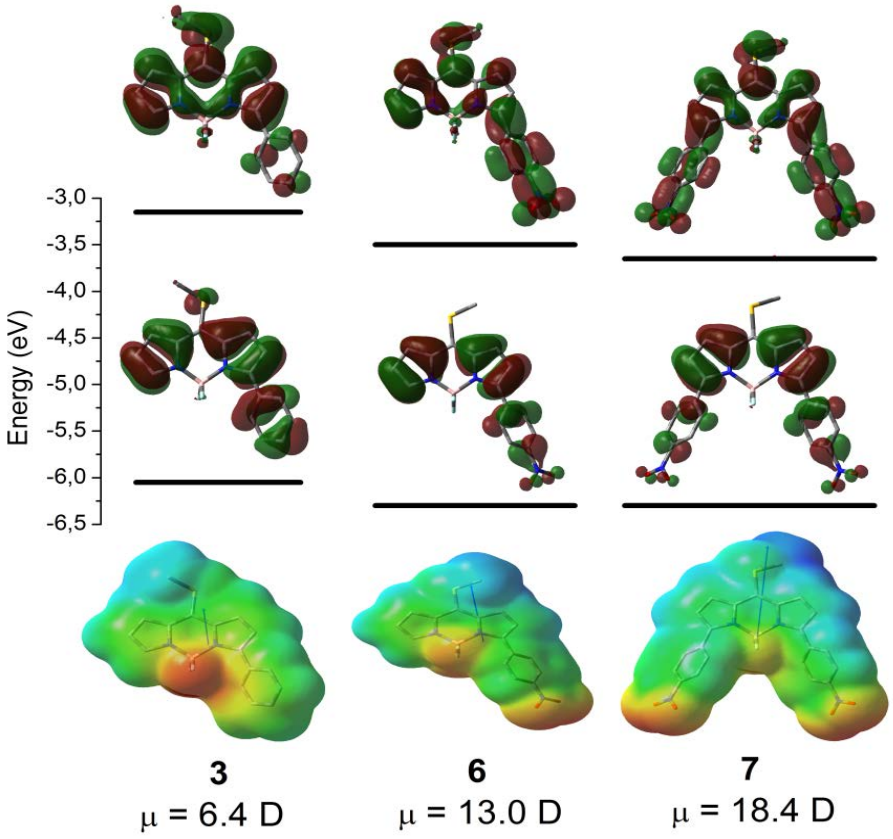

Fig. 4. Contour maps and energy of the frontier molecular orbitals (HOMO and LUMO) and electrostatic potential mapped onto the electronic density (positive in blue and negative in red) for representative 8-thiolated compounds **3**, **6** and **7**. The molecular dipole moment value and orientation in the ground state are also plotted.

The attachment of EW groups of different strengths (iodine, with σ_p^+ = 0.14, in compound **5**; carboxilate, with σ_p^+ = 0.42, in **4**; and nitro, with σ_p^+ = 0.79, in **6,** see Chart 1) at the *para* position of the 3-phenyl has no significant impact in the spectral band position (HOMO and LUMO are stabilized in a similar manner, Fig. 4), but it has a remarkable influence in the fluorescence response (Table 2). Thus, the higher the EW ability of such substituent, the higher are the reached fluorescence quantum yield and lifetime. Even the heavy iodine atom shows reasonable fluorescence efficiencies (up to 53%) in spite of its known promotion of intersystem crossing. Moreover, the above claimed dependency of such fluorescence parameters with the solvent properties is clearly diminished, suggesting that the ICT formation is decreased with such functionality. High fluorescence efficiencies have been previously reported for related 3-mono and 3,5-diarylated BODIPYs bearing EW cyano and nitro moieties at the *para* position, but without ED groups at position 8 [4a,6]. This is why the herein reported results are rather surprising and unexpected since these **4**-**6** dyes have a marked push-pull character (from position 8 to position 3) as reflected in the noticeable increase of the molecule dipole moment along the transversal axis (Fig. 4). Indeed dyes **4** and **6** have dipoles of about 13 Debyes (even in the LE state), with the positive charge located around the *meso*-methylthio group and the negative one shared between the fluorine atoms and the nitro group or the carboxilate group, respectively, at the opposite position. This trend anticipates a high charge separation and hence, it should enhance the ICT formation, with the consequent loss of fluorescence signal. However, this ED and EW combination renders the opposite behavior and strongly fluorescence polar dyes are achieved. Indeed, the corresponding contour maps of the frontier orbitals reveal that, albeit a transfer of electronic density takes place from the dipyrrin to the nitro moiety

upon going from the HOMO to the LUMO, both are spread across the 3-position (see dye **6** in Fig. 4), given a fully delocalized π-system through the whole molecule. In contrast, in its counterpart **3**, such spread was much more noticeable in the HOMO and the electronic density in the LUMO was concentrated in the dipyrrin core, being residual the contribution of the aryl fragment. These trends support the suppression of the ICT in the push-pull chromophores **4**-**6**, which outstand as highly fluorescent dyes (up to 72% in Table 2 for dye **6**). In fact, the high fluorescence of the nitrated compound **6** is rather astonishing and unexpected. In a previous work, we reported that the direct linkage of a nitro moiety to the dipyrrin core was deleterious for the fluorescence of 8-arylated and alkylated BODIPYs (reaching a fluorescence quantum yield of just 17% in the best case upon attachment of the nitro group directly at 3-position) [20]. Indeed, the induced ICT from the BODIPY core to the nitro group quenched the fluorescence emission from the former being almost negligible in polar media. However, the linkage of the nitro to the dipyrrin, bearing the 8-methylthio fragment, through a phenyl spacer seems to switch off such ICT, attending to the results collected in Table 2, and thus bright fluorophores are achieved.

In view of such encouraging results and as a proof of concept, we synthesized the corresponding analog double substituted with *para*-nitrophenyl groups at the symmetric 3- and 5-positions (dye **7** in Chart 1). The fully extended π-system of this dye pushes the spectral bands towards the red-edge of the visible (emission placed at around 620 nm, Fig. 5), owing to a LUMO stabilization (Fig. 4), keeping a bright fluorescence signal regardless of the polarity of the media (around 70%, Table 2) and in spite of the two strong EW nitro groups decorating the chromophore. Indeed, this dye is so polar (dipole moment around 18 D and reaching 20 D upon excitation) that the fluorescence band is clearly

bathochromically shifted (8 nm) with the solvent polarity, opposite trend to the typical negative solvatochromism in BODIPYs (Table 2). Therefore, the polar compound **7** is highlighted as a red-emitting push-pull dye (approaching the so-called biological window) endowed with strong fluorescence and suitable as molecular probe since the substituents at both 1- and 8-positions allow further postfunctionalization, as demonstrated in the previous section (for example LSCC and S_N reactions at the *meso* position activated by the 8-thiomethyl), to promote its selective recognition of an specific biomolecule.

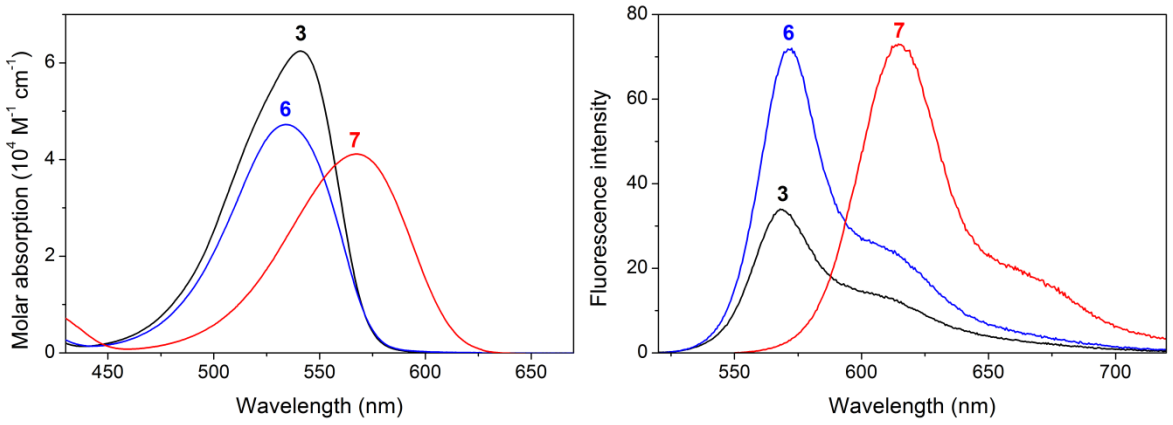

Fig. 5. Absorption and fluorescence (scaled by the fluorescence efficiency) spectra of dye **3** and its nitrated analogs **6** and **7** in cyclohexane. All the corresponding spectra of compounds **3**-**7** in this solvent are collected in Figure S1 in Supporting Information.

*3.2.2. Dyes **9**-**17**: 8-substituted 3-para-nitrophenylBODIPYs*

In view of the aforementioned encouraging results from the point of view of fluorescence, and to get deeper insight of the influence of the push-pull character from the 8-position to the 3-position on the photophysical signatures (mainly in its ability to induce ICT), we proceeded to systematically change the substituent at 8-position (in terms on its ED ability) keeping the same EW *para*-nitrophenyl arm at 3-position.

Those compounds featuring a constrained 8-aryl ring (phenyl bearing *ortho*-methyl **13** or *ortho*-methylenazide **15**, and naphthalene **17**, see Chart 3) or 8-acac (**12** in Chart 2)

display high fluorescence efficiencies in the tested solvents (up to 83%, Table 3) being similar to those achieved for their 8-thiolated counterpart **6** (see Table 2). Indeed, the steric hindrance induced at the 8-aryl (twisted around 70-78º with regard to the dipyrrin plane both in the ground and excited state) together with the weak ED ability of such rings or alkyls explain the low impact of such functionalization in the spectral band positions (see representative dye **13** in Fig. S2 in Supporting Information) as well as the absence of any negative influence on the fluorescence response related to the aryl free motion or ICT pathways, ensuing high fluorescence response in spite of the presence of the strong EW nitro group which endows a high polarity to the molecule (dipole moment up to 13 D). Nevertheless, a slight decrease of the fluorescence efficiency is recorded just for dye **12** bearing 8-acac in acetonitrile (Table 3), which was attributed to a specific interaction upon ionization of the enol form in basic media as observed previously [4b].

Table 3.

Photophysical data of dyes **9**-**17** in apolar (cyclohexane) and polar (acetonitrile) media. Full photophysical data are collected in Table S1 in Supporting Information.

		λ_{ab} (nm)	$\varepsilon_{max} \cdot 10^{-4}$ ($M^{-1}cm^{-1}$)	λ_{fl} (nm)	ϕ	τ (ns)
9[a]	c-hex	449.5	2.5	521.0	0.72	4.24
	ACN	427.5	2.3	522.5	0.07	0.20(24%)-0.94(76%)
12	c-hex	539.5	6.9	559.0	0.82	5.48
	ACN	536.5	3.3	561.0	0.57	5.88
13	c-hex	532.5	7.7	554.0	0.83	5.27
	ACN	529.0	6.7	557.0	0.79	5.59
14	c-hex	529.5	6.9	551.5	0.27	2.14
	ACN	525.5	5.6	555.0	0.12	0.82(98%)-3.50 (2%)
15	c-hex	534.5	6.7	556.5	0.82	5.38
	ACN	531.5	4.9	558.5	0.70	5.75
16	c-hex	530.5	3.6	572.5	0.35	2.73
	ACN	524.5	2.9	-	0.00	-
17	c-hex	536.5	7.4	559.5	0.78	5.28
	ACN	534.0	5.7	561.0	0.63	5.08

[a]for the 8-aminoBODIPYs dye **9** is chosen as representative (for full data see Table S1)

In contrast, those dyes bearing flexible *para*-substituted aryls with strong ED groups (methoxy with σ_p^+ = -0.31 in dye **14** and diphenylamine with σ_p^+ = -0.22 in **16**, see Chart 3) render much lower fluorescence efficiencies. The free motion of the 8-aryl (twisting dihedral angle down to 50º in ground state, increasing to 60º in LE) is known to efficiently quench the emission from the BODIPY [3]. In this regard, the substitution at the key 3-position counterbalances, at least to some extent, such non-radiative deactivation pathway as reflected in the attained fluorescence efficiencies in apolar media which, albeit low (up to 35% in dye **16**, Table 3), are higher than the expected ones for non-constrained 8-arylBODIPYs (usually lower than 10%) [3]. However, an increase of the solvent polarity results in a loss of the fluorescence signal, together with faster lifetimes (see dye **14** in Table 3). In particular, in compound **16**, with the highest charge separation (dipole moment up to 17 D), and hence bearing a more pronounced push-pull character, the emission is completely vanished (Table 3) owing to the excitation induced ICT. Indeed, it is known that the high ED ability of both groups, *p*-methoxyphenyl and mainly the electron rich triphenylamine, leads to strong fluorescence quenching when placed at *meso* position [3]. In our case, the generated ICT is further magnified by the presence of the EW nitro group at the opposite 3-position, explaining the absence of fluorescence signal for compound **16** in polar media. Moreover, its contour maps (Fig. 6) envisage that the ICT seems to evolve into a photoinduced electron transfer (PET) which would further contribute to the complete lack of emission in polar media. In fact, the electron density of the HOMO is placed exclusively in the triphenylamine, thus being intercalated between the LUMO and HOMO-1 orbitals, which are located in the dipyrrin core and spread through the nitrophenyl arm. Indeed TD-DFT simulations indicate that now the main absorption transition takes place from the

HOMO-1 to the LUMO. In this energetic picture (confirmed also with the most sophisticated CAM-B3LYP functional) a reductive PET is thermodynamically feasible from the HOMO. However, this assumption derived from static calculations should be taken with care, since advanced dynamic calculations in the excited state have revealed that the underlying quenching mechanism in some putative PET is still a dark ICT populated through a conical intersection [21]. Taking into account the sensitivity of the fluorescence efficiency to the solvent polarity, the last explanation is likely more reliable.

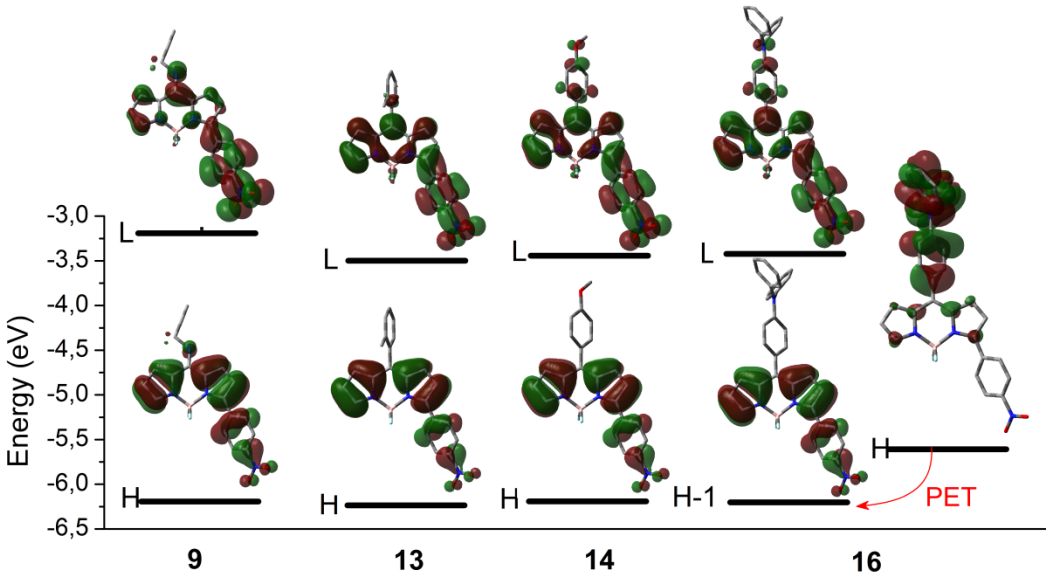

Fig. 6. HOMO (H) and LUMO (L) contour maps and energies of representative compounds of the 3-*p*-nitrophenylBODIPYs; dye **9** for 8-amino derivatives, dye **13** for those bearing sterically hindered 8-phenyls, and dyes **14** and **16** for derivatives bearing strong ED moieties at *para* position of unconstrained 8-phenyls. In the last dye the HOMO-1 (H-1) has been also included to account for a possible PET process.

The amine was also directly linked to the aforementioned *meso* position (dyes **9**-**11** bearing primary (σ_p^+ = -1.30) and secondary (σ_p^+ = -1.81) amines, see Chart 2). The corresponding spectral bands were shifted (mainly in absorption) to the blue edge of the visible spectrum (Table 3 and Figure S2 in Supporting Information) as result of the induction of a new hemicyanine-like π-system previously reported [22]. In our case the

additional presence of 3-nitrophenyl implies that the hemicyanine comprises a more extended π-system leading to a less pronounced hypsochromic shift. Again the high push-pull behavior of these dyes enables the dark ICT population, supporting the strong sensitivity of the fluorescence efficiency and lifetime to the solvent polarity (fluorescence efficiency drops from 60-70% to just 5-10% in polar solvents together with fast lifetimes from biexponential decays, Table 3). Similar evolutions were recorded for the BODIPY bearing 8-methylamine and were assigned as well to a photoinduced ICT [22]. However, the corresponding fluorescence response of the BODIPY bearing just primary amine at *meso* position showed no sensitivity to the solvent polarity (retaining values around 90%) [22]. Therefore, the presence of the EW 3-nitrophenyl arm strengths the push-pull behavior in dye **10,** thereby enhancing the ICT population. Indeed, the claimed shift of electronic density from the dypirrin to the nitrophenyl upon excitation is much clearer when amine is directly attached to the *meso* position (see dye **9** in Fig. 6). The contribution of the dipyrrin core to the LUMO is rather low and the electronic density in this orbital is mainly located along the 3-nitrophenyl unit. Such higher charge transfer upon excitation would explain also that the 8-amino induced hypsochromic shift is much lower at the fluorescence band than at the absorption one (Figure S2 in Supporting Information).

Therefore, all this set of compounds is endowed with high charge separation and can be classified as push-pull chromophores. On one hand, those dyes with the softer ED moiety at position 8 display high fluorescence response. On the other hand, the fluorescence efficiency of the compounds bearing strong ED motifs at the said *meso* position is triggered by a low-lying non-emissive ICT state, mainly in polar media. Nonetheless, the nitro group does not damage the fluorescence response as much as one

could expect in terms of its high EW ability, even in combination with ED moieties. Thus, adjusting the electron releasing ability of the group grafted at 8-position strongly fluorescent nitrated push-pull dyes can be developed.

*3.2.3. Dyes **20-23**: 8-substituted 3-para-aminophenylBODIPYs*

Once checked the impact of the EW nitro functionalization at position 3, we decided to replace it by the ED amine in some of the aforementioned compounds. In particular in those dyes bearing sterically hindered aryl groups (dyes **13** and **17)** and electron donor moieties (**14** and **16)** at 8-position, giving rise to dyes **20** and **23**, **21** and **22**, respectively (see structures in Chart 5 and their photophysical properties collected in Table S2 in Supporting Information). Note that in these compounds the BODIPY acts as electron acceptor (reverse situation than in the preceding section with nitrated BODIPYs), and, that in the last pair of compounds the core is decorated with two ED moieties leading to D-A-D structures [23].

The electron releasing ability of such amines at the *para* position of the 3-phenyl provides further bathochromic shift of the absorption band than the corresponding nitrated analogs in apolar media (around 30-35 nm, see Figure S3-S4 in Supporting Information). Dye **20**, bearing 8-*o*-methylphenyl**,** displays quite high fluorescence efficiency in apolar media but such emission almost completely disappears in polar media (Fig. 7), where the decay becomes biexponential owing to the appearance of a short lifetime of around 1 ns (Table S2 in Supporting Information), suggesting that it undergoes an efficient and non-emissive ICT process. Indeed, albeit the dipole moment is low in these 3-amino derivatives (just 5 D), the corresponding frontier molecular orbitals foresee their tendency to induce charge transfer since the hop from the HOMO to the LUMO implies a shift of electronic

density from the amine to the dipyrrin core (Figure S5 in Supporting Information). It should be borne in mind that its corresponding nitrated analog **13** yielded high fluorescence signals regardless of the solvent polarity (Fig. 7). In other words, the BODIPY core behaves better as electron acceptor rather than donor. Therefore, the amine group greatly favors the formation of an ICT state, as observed previously in related push-pull chromophores bearing the said 3-amine and ED or EW groups at 8-position [6,24]. Nevertheless, it should be emphasized the main role of the 8-functionalization in the activation of the ICT, since the direct linkage of 3-amine to an alkylated BODIPY yielded high fluorescence efficiencies, without sign of ICT formation [20].

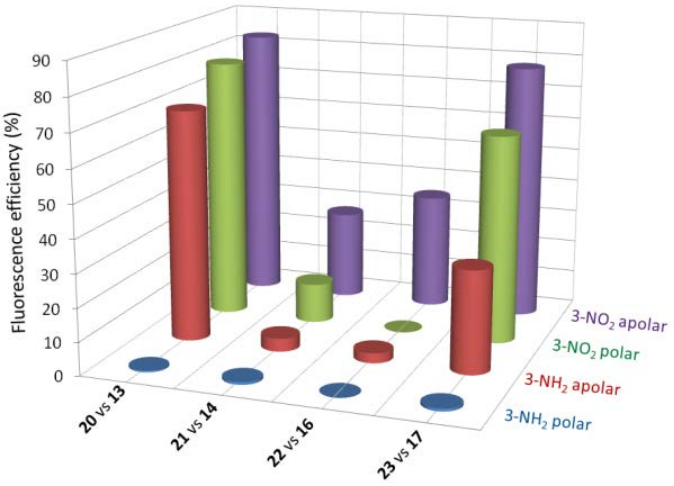

Fig. 7. Evolution of the fluorescence efficiency of the 3-amino dyes (**20**-**23**) and their 3-nitro counterparts (**13**, **14**, **16** and **17**) BODIPYs in apolar and polar solvents. For full photophysical data of the amino derivatives see Table S2 in Supporting Information.

The other constrained derivative **23**, featuring 8-naphthalene, shows a quite different fluorescence behavior with regard to its analog **20**. As a matter of fact, the fluorescence profile comprises two clearly distinguishable bands (Fig. 8). Accordingly to the presence of ICT processes induced by the 3-amine, the short-wavelength band (around 565 nm) is attributed to the expected emission from the LE state, but quenched by the

induced ICT, which in this case retains its own fluorescence emission at longer wavelengths (618 nm) and prevails in the fluorescence spectrum. This is why high Stokes shifts are recorded (up to 1500 cm^{-1}, Table S2 in Supporting Information) since the absorbing state (LE) differs from the emitting one (ICT). Likely, the naphthalene is better ED than the phenyl and further stabilizes the ICT formation, thus enabling its fluorescence emission at longer-wavelength and explaining the lower fluorescence efficiency in apolar media (Fig. 7).

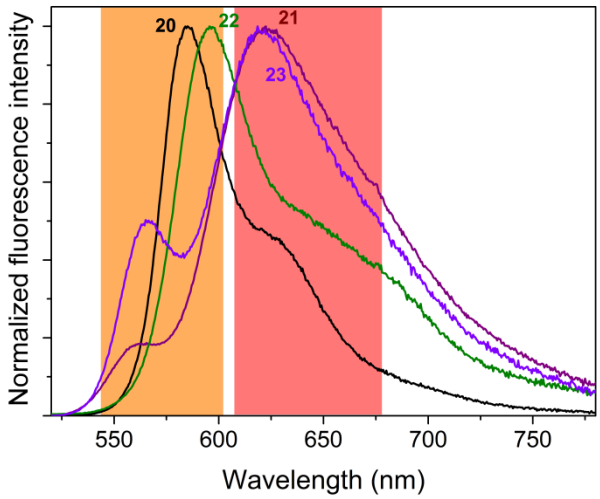

Fig. 8. Normalized fluorescence spectra of dyes **20**-**23** in apolar solvents. The two emission channels (from the LE state, orange shaded, and from the ICT state, red shaded) are highlighted.

Moreover, the fluorescence decay at the LE emission is monoexponential with a lifetime of 4.2 ns, whereas at the ICT emission maximum it becomes biexponential with a faster lifetime of 1.3 ns (Table S2 in Supporting Information). A further increase of the solvent polarity leads to a loss of such new emission, being the spectrum dominated by the LE emission but so quenched that the fluorescence signal is hardly detectable (Fig. 7). The dependency of the emission probability from the ICT with the polarity can be explained as follows. In polar media the charge separation of the ICT state is stabilized, being the

quenching of the emission from the LE state more pronounced. However, at the same time the charge recombination required to detect its emission, is less feasible and the non-radiative relaxations from the ICT increases in detriment of its own fluorescent deactivation [25]. Moreover, it has been previously reported that in some dyes where the ICT is very stabilized by structural and environmental reasons, it can evolve into a dark charge separation (CS) state giving rise to a complete loss of fluorescence [26]. It should be noted that again the nitro-containing counterpart **17** was strongly fluorescent in all tested solvents (Fig. 7).

As consequence of the D-A-D structure of the dyes **21** and **22** (8-*p*-methoxyphenyl and 8-triphenylamine, respectively, plus the 3-aminophenyl), the fluorescence response of both is almost negligible even in apolar media (Fig. 7). Thus, the ICT is again much more evident than in their nitro-containing counterparts **14** and **16.** In analogy to dye **23** in apolar solvents, the ICT state of both D-A-D dyes shows weak emission at long-wavelengths (clearer in **21** than in **22**, where it is just a shoulder, Fig. 8) but it tends to disappear in more polar media as happens also with the LE emission. Again the electron rich triphenylamine grafted at *meso* position seems to induce PET processes since two energetically close-lying occupied orbitals are proposed, in which the electronic density is placed preferably in both donor moieties (see D-A-D dye **22** in Fig. S5 in Supporting Information). Furthermore, in these last dyes the ICT appears to be so favored by amination that it seems to be already formed in the ground state, at least in polar media. This statement is supported by several facts taking as reference dye **20**: (i) the absorption band position shifts bathochromically with the solvent polarity, in contrast to the expected hypsochromic shift in BODIPYs (Table S2 in Supporting Information); (ii) the change from cyclohexane to acetonitrile entails a broadening of the absorption profile (Fig. 9); (iii) the excitation spectrum does not

match the whole absorption band, just the short-wavelength part (Fig. 9); and (iv) the fluorescence spectrum changes with the excitation wavelength (Fig. 9). Thus exciting at short wavelengths the expected LE emission is recorded, but exciting at long-wavelengths a very weak ICT emission is detected. All these trends support that the ICT can be populated not only from the LE state as a photoinduced process, but also directly because its own absorption is allowed. This fact explains the negative Stokes shift listed in Table S2 in Supporting Information since in polar media the contribution of the ICT to the whole absorption profile is higher (leading to the above mentioned apparent bathochromic shift). Similar ICT absorptions have been also addressed in other push-pull BODIPYs [27].

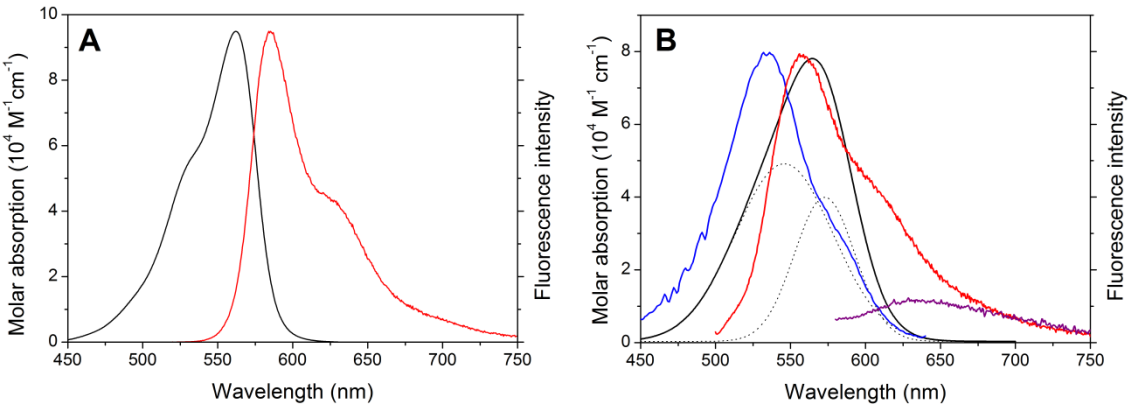

Fig. 9. Absorption (black) and normalized fluorescence (red) of dye **20** in ciclohexane (A) and acetonitrile (B). In this last solvent the excitation spectrum (λ_{em} = 650 nm, in blue) and the fluorescence spectra at different excitation wavelengths (490 nm in red and 570 nm in purple) are also included. The deconvolution of the absorption spectrum in acetonitrile in two gaussians (dotted black lines) is also plotted to account for the own absorption of the ICT.

Summing up, albeit the ICT promoted by the 3-amine has its own red-shifted fluorescence signal, it is rather weak and its quenching effect is highly effective in combination with EW moieties at 8-position or in polar media, leading to poorly

607 fluorescent push-pull dyes, in contrast to most of their nitrated analogs, which outstand by
608 their bright emission.
609
610 *3.2.4. Dyes **8, 18, 19** and **24**: influence of the chromophoric substitution position*
611 Finally, we wanted to gain deeper insight into the role of the position in which the
612 ED and EW moieties are grafted to the core. To this aim the *p*-nitrophenyl moiety (**8**, **18**
613 and **19**, see Chart 4), as well as the *p*-aminophenyl group (**24**, see Chart 5), were attached to
614 the 1-position of the 8-functionalized dipyrrin core methylated at 3- and 5-positions. Such
615 alkylation at those specific positions was previously tested as profitable for the fluorescence
616 response of BODIPYs bearing 8-heteroatoms (i.e. dye **1b**) [17] and flexible 8-aryls [3].
617 The *p*-nitrophenyl arm at 1-position does not interact by resonance with the dipyrrin
618 core as revealed by their corresponding HOMO contour maps (Fig. 10 and Fig. S6 in
619 Supporting Information). Indeed, the twisting angle for such phenyl at 1-position (around
620 50º) is higher than in 3-position (around 30º) suggested that the former position has a
621 higher steric strain. As consequence, the absorption bands of 1-nitro compounds are
622 hypsochromically shifted with regard to their corresponding 3-nitro analogs (see for
623 example compounds **19** vs **13** in Fig. 10, and Table S1 and S2 in Supporting Information
624 for nitro and amino derivatives, respectively). Note that the methyl groups at 3- and 5-
625 positions counterbalance in part such shift to higher energies owing to their positive
626 inductive effect. Furthermore, the *p*-aminophenyl rest in dye **24** neither shifts the absorption
627 band excluding any resonant interaction. At this point, there is a mismatch with the
628 theoretical calculations, as they predict an extended delocalization through the aminophenyl
629 moiety (even the more advanced CAM-B3LYP functional predicts such apparent resonant
630 interaction). Such disparity can rely on the two energetically close (just 0.3 eV) occupied

orbitals with induce the extra presence of the 8-triphenylamine. Likely, the simulation is not able to completely separate both orbitals and there is some degree of mixing in the assignment of the electronic density corresponding to each one. Attending to the experimental finding the resonant interaction promoted by the 1-amine should be rather low since it is not reflected in the ensuing bathochromic shift (Table S2 in Supporting Information).

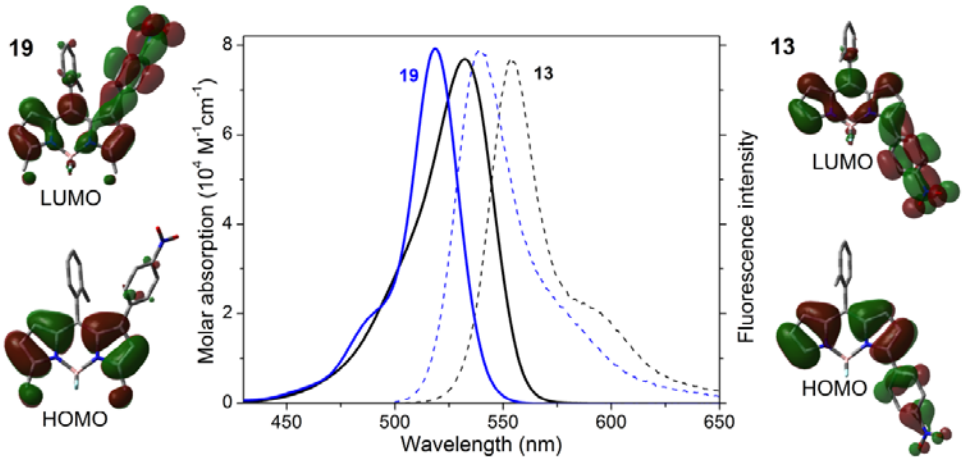

Fig. 10. Absorption (solid line) and normalized fluorescence (dashed lines) spectra of dyes **13** and **19** in cyclohexane. The corresponding contour maps of the frontier orbitals are also depicted.

High fluorescence efficiencies are attained for the 1-nitro dye **19** bearing the less ED moiety at 8-position (*o*-methylphenyl in **19**) in apolar media (Fig. 11 and Table S1 in Supporting Information). However, further increase of the solvent polarity leads to a pronounced loss of the fluorescence response, which is again attributed to the promotion of an ICT state by the non-conjugated 1-nitrophenyl group. In particular, such ICT points to a twisted one (TICT) owing to the exerted geometrical tensions by the spatial proximity of the aryl groups at 1- and 8-position. Indeed, a clear shift of electronic density from the dipyrrin core to the nitrophenyl is predicted going from the HOMO to the LUMO, since in the last state the contribution of the aromatic substituent at 1-position is much more

noticeable (Fig. 10). Note that the same substitution at 3-position provided high fluorescence signal regardless of the solvent (Fig. 11), postulating the last chromophoric position as suitable to enhance the fluorescence efficiency, while the former is recommended to induce charge separation upon excitation and ICT pathways.

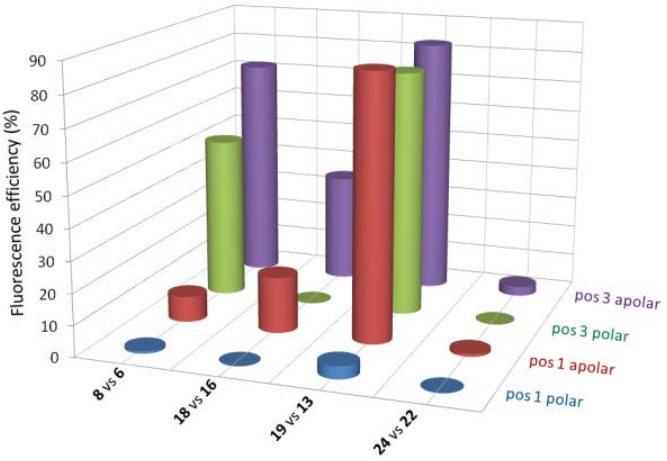

Fig. 11. Evolution of the fluorescence efficiency of the 1-substituted dyes (**8, 18, 19** and **24**) and their 3-substituted counterparts (**6**, **16**, **13** and **22**) in apolar and polar solvents. For full photophysical data of the nitro and amino derivatives see Table S1 and S2, respectively in Supporting Information.

An increase of the ED ability of the substituent at 8-position (methylthio group in dye **8** and triphenylamine moiety in dye **18**) is detrimental for the fluorescent efficiency of 1-nitro compounds, and their emission becomes almost entirely suppressed in polar media (Fig. 11 and Table S1 in Supporting Information). As a matter of fact, a TICT state was also claimed to explain the absence of fluorescence signal in a constrained alkylated analog of the thiolated dye **8,** in particular, dye **1b** with additional methyl groups at 1- and 7-positions [17]. Moreover, attending to the high Stokes shift of dye **18** (up to 2100 cm^{-1} in Table S1 in Supporting Information), it is stated that the emission comes mainly from the ICT state, with a short-wavelength shoulder attributed to the emission from the LE state (Fig. S7 in Supporting Information). Again, the corresponding counterparts with the EW

nitro moiety at 3-position show much higher fluorescence efficiency, mainly in apolar media (Fig. 11). Furthermore, the ability of the strong ED and electron rich triphenylamine to induce ICT processes enables a putative PET process, as drawn out from the theoretical simulations of the molecular orbitals (Fig. S6 in Supporting Information), in line with the results above described for related 8-triphenylamineBODIPYs.

The replacement of the EW nitro group at 1-position by the ED amine (dye **24**) leads to a drastic loss of the fluorescence signal, in agreement with the aforementioned higher ability of the amine to induce ICT in BODIPYs (see for example dye **22**), especially if the electron rich triphenylamine is also placed at 8-position. Again, the molecular orbitals suggest that again a PET pathway could take place from both ED moieties to the BODIPY (Fig. S6 in Supporting Information). As consequence, dye **24** becomes almost non-fluorescent in any of the tested solvents. Accordingly, the fluorescence profile in apolar media is dominated by a weak and long wavelength emission (Fig. S7 in Supporting Information) which is attributed again to the TICT on the basis of its high Stokes shift (up to 3000 cm^{-1} in Table S2 in Supporting Information). As expected, such emission disappears completely in polar media (Fig. 11). Moreover, whereas in dyes **8** and **19** the TICT is photoinduced since the absorption profile is sharp and similar to that typical of BODIPYs, we cannot rule out that in dyes **18** and **24**, with the strongest push-pull or D-A-D character, such TICT could be directly populated (as it happens in the above described 3-amino BODIPYs) since the corresponding spectra show a broadening at lower energies in polar solvents (see as example the growing at the long-wavelength tail for compound **18** in Fig. S8 in Supporting Information).

In brief, the insertion of ED or EW at 1-position greatly favors the ICT processes, especially in combination with ED moieties at 8-position, leading to poorly fluorescent

compounds, or at least with a fluorescence response very sensitive to the polarity of the surrounding environment.

4. Conclusions

Biellmann BODIPYs were prepared via a C-H arylation reaction with *in-situ* formed aryldiazonium salts. It was demonstrated that the MeS group of these new derivatives exhibited good reactivity in both S_NAr and cross-coupling reactions. Following this synthetic methodology the dipyrrin core has been decorated with electron rich or poor moieties in specific chromophoric positions leading to a wide pool of push-pull dyes involving 8- and 3-positions, or 8- and 1-positions. A rational design of such functionalization, in terms of the strength of the electron donor and withdrawing moieties, their simultaneous combination in the same structure and the position in which they are anchored, drastically modulates the photophysical signatures of BODIPYs giving rise to highly fluorescence dyes, suitable as laser dyes and molecular probes, or, alternatively to poorly fluorescence compounds, but endowed with high charge separation upon excitation, being potential candidates for non-linear optics or as photosensitizers in photovoltaic devices. The key factor is the possibility to adjust the ICT probability via the right substitution pattern since such process triggers the fluorescence efficiency. Thus, searching for highly fluorescence dyes, the combination of soft electron donors anchored at 8-position (such as constrained aryl, alkyl or methylthio moieties) with strong electron withdrawing nitro groups at 3-position is successful. These push-pull dyes outstand by its bright emission regardless of the surrounding environment. Besides, their spectral bands can be pushed deeper towards the red edge upon additional nitration at the equivalent 5-position. On the other hand, the introduction of stronger electron donor moieties at 8-position (amino

or methoxy moieties), as well as the replacement of nitro by an amino group switches on a quenching ICT state which suppresses drastically the emission mainly in polar media, where the dye becomes non-fluorescent (mainly in D-A-D structures). Moreover, the functionalized chromophoric position plays also a critical role since bright fluorophores or opposite "dark" compounds are attained with the same substituents but just changing the attachment position (3 or 1, respectively) at the chromophoric backbone.

Therefore, the herein reported work provides key structural guidelines to settle and understand the impact of the substitution pattern in the photophysical properties, which should orient the development of new fluorophores with tailor-made properties. As a matter of fact, we have demonstrated that, after a rational design, the usually low fluorescence response of the push-pull chromophores can be overcome, thereby leading to BODIPYs with high charge separation, as reflected in the molecular dipole moments, but keeping a high fluorescence signal.

Acknowledgments

We thank CONACyT (grants 253623, 123732), Gobierno Vasco (IT912-16) and Spanish MICINN (MAT2014-51937-C3-3-P) for financial support. J. L. B.-V. and L. B.-M. thank CONACyT for graduate scholarship. R.S.-L. thanks UPV-EHU for a postdoctoral fellowship. Donation of Biellman BODIPYs by Cuantico de Mexico (www.cuantico.mx) is appreciated.

Appendix A. Supplementary data

740 Characterization data and copies of both ^{1}H and ^{13}C NMR spectra of all of the compounds
741 in this paper. Complementary photophysical data as well as results from theoretical
742 calculations in Tables S1-S2 and Figures S1-S8.
743
744 **References**

745 [1] Goud TV, Tutar A, Biellmann JF. Synthesis of 8-heteroatom-substituted 4,4-difluoro-
746 4-bora-3a,4a-diaza-s-indacene dyes (BODIPY). Tetrahedron 2006; 62: 5084-91.
747 [2] (a) Ulrich G, Ziessel R, Harriman A. The chemistry of fluorescent bodipy dyes:
748 versatility unsurpassed. Angew. Chem. Int. Ed. 2008; 47: 1184-201.
749 (b) Loudet A, Burgess K. BODIPY dyes and their derivatives: syntheses and
750 spectroscopic properties. Chem. Rev. 2007; 107: 4891-932.
751 (c) Ziessel R, Ulrich G, Harriman A. The chemistry of Bodipy: A new *El Dorado* for
752 fluorescence tools. New J. Chem. 2007; 31: 496-501.
753 (d) Lu H, Mack J, Yang Y, Shen Z. Structural modification strategies for the rational
754 design of red/NIR region BODIPYs.Chem. Soc. Rev. 2014; 43. 4778-823.
755 (e) Boens N, Leen V, Dehaen W. Fluorescent indicators based on BODIPY. Chem.
756 Soc. Rev. 2012; 41: 1130-72.
757 (f) Kowada T, Maeda H, Kikuchi K. BODIPY-based probes for the fluorescence
758 imaging of biomolecules in living cells. Chem. Soc. Rev. 2015; 44. 4953-72.
759 [3] Betancourt-Mendiola L, Valois-Escamilla I, Arbeloa T, Bañuelos J, López-Arbeloa I,
760 Flores-Rizo JO, et al. Scope and limitations of the Liebeskind-Srogl cross-coupling
761 reaction involving the Bielmann BODIPY. J. Org. Chem. 2015; 80: 5771-82, and
762 references therein.

763 [4] (a) Gómez-Durán CFA, Esnal I, Valois-Escamilla I, Urías-Benavides A, Bañuelos J,
764 López-Arbeloa I, et al. Near-IR BODIPY dyes à la carte – programmed orthogonal
765 functionalization of rationally designed building blocks. Chem. Eur. J. 2016; 22:
766 1048-61.
767 (b) Gutiérrez-Ramos BD, Bañuelos J, Arbeloa T, López-Arbeloa I, González-Navarro
768 PE, Wrobel K, et al. Straightforward synthetic protocol for the introduction of
769 stabilized C nucleophiles in the BODIPY core for advanced sensing and photonic
770 applications. Chem. Eur. J. 2015; 21: 1755-64.
771 [5] Thivierge C, Bandichhor R, Burgess, K. Spectral dispersion and water solubilization
772 of BODIPY dyes via palladium-catalyzed C-H functionalization. Org. Lett. 2007; 9:
773 2135-38.
774 [6] Verbelen B, Boodts S, Hofkens J, Boens N, Dehaen W. Radical C-H arylation of the
775 BODIPY core with aryldiazonium salts: synthesis of highly fluorescent red-shifted
776 dyes. Angew. Chem. Int. Ed. 2015; 54: 4612-6.
777 [7] Verbelen B, Dias Rezende LC, Boodts S, Jacobs J, Van Meervelt L, Hofkens J,
778 Dehaen W. Radical C-H alkylation of BODIPY dyes using potassium trifluoroborates
779 or boronic acids. Chem. Eur. J. 2015; 21: 12667-75.
780 [8] (a) Liu Y, Li Z, Chen L, Xie Z. Near infrared BODIPY-Platinum conjugates for
781 imaging, photodynamic therapy and chemotherapy. Dyes and Pigments. 2017; 141:
782 5-12.
783 (b) Gao M, Yu F, Chen H, Chen L. Near-infrared fluorescent probe for imaging
784 mitochondrial hydrogen polysulfides in living cells and in vivo. Anal. Chem. 2015;
785 87:3631-8.

(c) Gao M, Wang R, Yu F, You J, Chen L. A near-infrared fluorescent probe for the detection of hydrogen polysulfides biosynthetic pathways in living cells and in vivo. Analyst 2015; 140; 3766-72.

(d) Liu P, Jing X, Yu X, Lv C, Chen L. A near-infrared fluorescent probe for the selective detection of HNO in loving cells and in vivo. Analyst 2015; 140: 4576-83.

(e) Jing X, Yu F, Chen L. Visualization of nitroxyl (HNO) in vivo via a lysosome-targetable near-infrared fluorescente probe. Chem. Commun. 2014; 50: 14253-6.

(f) Ni Y, Wu, J. Far-red and near infrared BODIPY dyes: synthesis and application for fluorescent pH probes and bio-imaging. Org. Biomol. Chem. 2014; 12: 3774-91.

(g) Shandura, M. P.; Yakubovskyi, V.P.; Gerasov, A. O.; Kachkovsky, O. D.; Poronik, Y. M.; Kovtun, Y. P. α-Polymethylene-susbtituted bron dipyrromethenes – BODIPY-based NIR cyanine-like dyes. Eur. J. Org. Chem. 2012; 1825-34.

(h) Tasior, M.; O'Shea, D. F. BF_2-chelated tetraarylazadipyrromethenes as NIR fluorochromes. Bioconjugate Chem. 2010; 21: 1130-33.

[9] (a) Qiang G; Wang ZY. Near-infrared organic compounds and emerging applications. Chem. Asian J. 2010; 5: 1006-29.

(b) Kubo Y, Watanabe K, Nishiyabu R, Hata R, Murakami A, Shoda T, et al Near-infrared absorbing boron-dibenzopyrromethenes that serve as light-harvesting sensitizers for polymeric solar cells. Org. Lett. 2011; 13: 4574-77.

(c) Galangau O, Dumas-Verdes C, Méallet-Renault R, Clavier G. Rational design of visible and NIR distyryl-BODIPY dyes from a novel fluorinated platform. Org. Biomol. Chem. 2010; 8: 4546-53.

(d) Donuru VR, Zhu S, Green S, Liu H. Near-infrared emissive BODIPY polymeric and copolimeric dyes. Polymer 2010; 51: 5359-68.

[10] (a) Xuan S, Zhao N, Ke X, Zhou Z, Fronczek FR, Kadish KM, et al. Synthesis and spectroscopic investigation of a series of push-pull boron-dipyrromethenes (BODIPYs). J. Org. Chem. 2017; 82; 2545-57.

(b) Jian X-D, Liu X, Fang T, Sun C. Synthesis and application of methylthio-substituted BODIPYs/aza-BODIPYs. Dyes and Pigments. 2017; 146: 438-44.

(c) Poddar M, Gautam P, Rout Y, Misra R. Donor-acceptor phenothiazine functionalized BODIPYs. Dyes and Pigments. 2017; 146: 368-73.

(d) Petrushenko KB, Petrushenko IK, Petrova OV, Sobenina LN, Trofimov BA. Dyes and Pigments. 2017; 136: 488-95.

[11] (a) Bessette A, Hanan GS. Design, synthesis and photophysical studies of dipyrromethene-based materials: insights into their applications in organic photovoltaic devices. Chem. Soc. Rev. 2014: 4; 3342-405.

(b) Singh SP, Gayathri T. Evolution of BODIPY dyes as potential sensitizers for dye-sensitized solar cells. Eur. J. Org. Chem. 2014; 4689-707.

[12] (a) Kulyk B, Taboukhat S, Akdas-Kilig H, Fillaut J-L, Kapierz M, Sahraoui B. Tuning the nonlinear optical properties of BODIPYs by functionalization with dimethylaminostyryl substituents. Dyes and Pigments. 2017; 137: 507-11.

(b) Frenette M, Hatamimoslehabadi M, Bellinger-Buckley S, Laoui S, Bab S, Dantiste O, et al. Nonlinear optical properties of multipyrrole dyes. Chem. Phys. Lett. 2014; 608: 303-7.

[13] (a) Küçüköz B, Sevinç G, Yildiz E, Karatay A, Zhong F, Yilmaz H, et al. Enhancement of two photon absorption properties and intersystem crossing by charge

832 transfer in pentaaryl boron-dipyrromethene (BODIPY) derivatives. Phys. Chem.
833 Chem. Phys. 2016; 18: 13546-53.
834 (b) Zhang X, Xiao Y, Qi J, Qu J, Kim B, Yue B, et al. Long-wavelength, photostable,
835 two-photon excitable BODIPY fluorophores readily modifiable for molecular probes.
836 J. Org. Chem. 2013; 78: 9153-60.
837 [14] Oger N, d'Halluin M, Le Grognec E, Felpin FX. Using aryl diazonium salts in
838 palladium-catalyzed reactions under safer conditions. Org. Process Res. Dev. 2014;
839 18: 1786-801.
840 [15] Pinacho-Crisóstomo F, Martín T, Carrillo R. Ascorbic acid as an initiator for the
841 direct C-H arylation of (hetero)arenes with anilines nitrosated in situ. Angew. Chem.
842 Int. Ed. 2014; 53: 2181-5.
843 [16] Peña-Cabrera E, Aguilar-Aguilar A, Gonzalez-Dominguez M, Lager E, Zamudio-
844 Vazquez R, Godoy-Vargas J, et al. Simple, general, and efficient synthesis of meso-
845 substituted borondipyrromethenes from a single platform. Org. Lett. 2007; 9: 3985-
846 88.
847 [17] Li Q, Guo Y, Shao S. A BODIPY derivative as a highly selective "off-on"
848 fluorescente chemosensor for hydrogen sulfate anion. Analyst, 2012; 137: 4497-501.
849 [18] Esnal I, Valois-Escamilla I, Gómez-Durán CFA, Urías-Benavides A, Betancourt-
850 Mendiola ML, López-Arbeloa I, et al. Blue-to-orange color-tunable laser emission
851 from tailored boron-dipyrromethene dyes. ChemPhysChem 2013; 14: 4134-42.
852 [19] Corwin H, Leo A, Taft RW. A survey of Hammett substituent constants and
853 resonance and field parameters. Chem. Rev. 1991; 91: 165-95.

[20] Esnal I, Bañuelos J, López-Arbeloa I, Costela A, Garcia-Moreno I, Garzón M, et al. Nitro and amino BODIPYs: crucial substituents to modulate their photonic behavior. RSC Adv. 2013; 3: 1547-56.

[21] Escudero D. Revising intramolecular photoinduced electron transfer (PET) from first-principles. Acc. Chem. Res. 2016; 49: 1816-24

[22] Bañuelos J, Martin V, Gómez-Durán CFA, Arroyo-Córdoba IJ, Peña-Cabrera E, García-Moreno I, et al. New 8-amino-BODIPY derivatives: surpassing laser dyes at blue-edge wavelengths. Chem. Eur. J. 2011; 17: 7261-70.

[23] Liao J, Zhao H, Xu Y, Cai Z, Peng Z, Zhang W, et al. Novel D-A-D type dyes based on BODIPY platform for solution processed organic cells. Dyes and Pigments. 2016; 128: 131-40.

[24] (a) Ganapathi E, Madhu S, Chaterjee T, Gonnade R, Ravikanth M. Synthesis, structure, spectral, electrochemical and sensing properties of 3-amino boron-dipyrromethene and its derivatives. Dyes and Pigments 2014; 102: 218-27.

(b) Petrushenko KB, Petrushenko IK, Petrova OV, Sobenina LN, Ushakov IA, Trofimov BA. Environment-responsive 8-CF_3-BODIPY dyes with aniline groups at the 3 position: synthesis, optical properties and RI-CC2 calculations. Asian J. Org. Chem. 2017; DOI:10.1002/ajoc.201700117.

[25] (a) Kollmannsberger, M., Rurack, K.; Resch-Genger, U.; Daub, J. *J. Phys. Chem. A* **1998**, *102*, 10211-10220.

(b) Nano, A.; Ziessel, R.; Stachelek, P.; Harriman, A. *Chem. Eur. J.* **2013**, *19*, 13528-13537.

[26] (a) Benniston AC, Clift S, Hagon J, Lemmetyinen H, Tkachenko NV, Clegg W, et al. Effect on charge transfer and charge recombination by insertion of a naphthalene-

based bridge in molecular dyads based on borondipyrromethene (Bodipy). ChemPhysChem 2012; 13: 3672-81.

(b) Gautam P, Misra R, Thomas MB, D´Souza F. Ultrafast charge-separation in triphenylamine-BODIPY-derived triads carrying centrally positioned, highly electron deficient, dicyanoquinodimethane or tetracyanobutadiene electron-acceptors. Chem. Eur. J. 2017; DOI: 10.1002/chem.201701604.

[27] Ziessel R, Retailleau P, Elliot KJ, Harriman A. Boron dipyrrin dyes exhibiting “push-pull-pull” electronic signatures. Chem. Eur. J. 2009; 15: 10369-74.